




Non-contact, highly sensitive sugar concentration detection based on $\text{Co}_3\text{Sn}_2\text{S}_2$ Weyl semimetal thin film sensor by terahertz wave

HONGYI LIN,¹  ZICHEN ZHANG,¹ FEILONG GAO,² JIANJIAN RUAN,¹ DONG SUN,¹ SHAODONG HOU,³  BINGYUAN ZHANG,^{2,4} AND QI SONG^{2,5} 

¹School of Optoelectronic and Communication Engineering, Xiamen University of Technology, Xiamen 361024, China

²Shandong Key Laboratory of Optical Communication Science and Technology, School of Physics Science and Information Technology, Liaocheng University, Liaocheng 252059, China

³Changzhou Inno Machining Co., Ltd. No.18-69, Changzhou 213164, China

⁴zhangbingyuan@lcu.edu.cn

⁵songqi@lcu.edu.cn

Abstract: Blood sugar is an important biomedical parameter of diabetic patients. The current blood sugar testing is based on an invasive method, which is not very friendly for patients who require long-term monitoring, while the non-invasive method is still in the developing stage. In this paper, we design a non-invasive and highly sensitive terahertz wave detector with $\text{Co}_3\text{Sn}_2\text{S}_2$ semimetal thin film to test sugar concentration. As different concentrations have inconsistent responses to terahertz wave, we can deduce the concentration of the sugar solution to realize real-time highly sensitive detection of blood sugar concentration. This novel method can be further expanded to 6 G edge intelligence for non-invasive and real-time monitoring of blood sugar, and promote the development of 6 G technology.

© 2024 Optica Publishing Group under the terms of the [Optica Open Access Publishing Agreement](#)

1. Introduction

According to the World Health Organization, the number of diabetic patients in the world has reached 537 million in 2023, and it will soon reach 634 million in 2030. Currently, blood sugar concentration is the key indicator for diagnosing diabetes. Diabetes is a long-term, incurable and chronic disease, which presents high incidence, numerous complications, a wide range of causative factors, treatment difficulty et al, and it causes serious harm to human health. So diabetic patients' priority is to control blood sugar stabilization, which requires patients to do timely blood sugar monitoring [1]. Based on whether blood sugar testing with skin and blood vessel lesions, it can be simply divided into invasive and non-invasive sugar testing [2]. Currently, both medical and household blood sugar meters belong to invasive sugar testing. This method is simple, accurate, speedy and cheap, but it requires to puncture veins or capillaries, and long-term testing poses a risk of infection and affect the patient health. Therefore, accurate, and rapid non-invasive blood sugar testing has become a current research hot issue.

Compared to traditional invasive testing means, the non-invasive testing is very convenient, which does not require skin puncture to collect a blood sample, and avoids the discomfort of pain and the risk of infection. It is continuous, safe, quick and practical for diabetic patients. Non-invasive sugar testing based on optical method is at the forefront of current research, such as infrared method [3], optical polarization method [4–8], Raman spectroscopy [9], optical coherence tomography [10], localized surface plasmon resonance (LSPR) [11], etc. As LSPR, Li et al. fabricated a graphene oxide/multiwalled carbon nanotubes assisted serial quadruple tapered

structure-based LSPR sensor for blood sugar detection. The sensitivity and limit of detection are 1.04 nm/mM and 0.24 mM at different sugar solutions of 0–10 mM, respectively [12]. However, all of these methods have some drawbacks. For example, the infrared method has the limitation of penetration depth, Raman spectroscopy has low sensitivity, and the resolution of optical coherence tomography is susceptible to scattering components. These above optical methods are often susceptible to external environment. Furthermore, the lack of standard parameters as a reference and individual differences can also affect the results. Therefore, current non-invasive blood sugar testing based on optical method often falls short of expectations.

Taking into account the above disadvantages, we have turned our attention to terahertz wave and utilized the terahertz response for non-invasive blood sugar testing. As the terahertz wave has a variety of characteristics such as penetrating and non-invasive, and it can easily penetrate the surface of the skin directly to the blood without the negative impact of the skin and blood vessels. Compared to other methods, terahertz wave is more sensitive to small signal and can visualize small changes, i.e., it is more accurate. In conclusion, terahertz wave has the potential of non-invasive testing and can overcome the shortcomings of the other methods mentioned above to a certain extent.

A good non-invasive blood sugar testing requires a high-performance detector, so the choice of the right material is essential. Here we consider Weyl semimetal, mainly due to its outstanding properties. In the Weyl semimetal, valence and conduction bands intersect at certain points in the Brillouin region, and then form a chiral Dirac cone. As the momentum of the crystal approaches the Dirac point, its energy level difference decreases until it reduces to zero. The band gap width is proportional to the displacement of the crystal momentum with respect to the Dirac point, and its unique energy level properties can be excited more efficiently by low-energy terahertz wave [13–14]. The absorption of terahertz photons by Weyl semi-metallic thin film creates electron-hole pairs, and then leads to the accumulation of carriers. Additionally, this material exhibits the characteristic of lower dark current and the Weyl point enhancement effect, so its Weyl point can reinforce the momentum of the carriers to achieve a stronger light current [15].

Furthermore, due to the unique electronic structure of the Weyl semimetal, it can exhibit excellent photo-detection performance in the terahertz range, so it can be used as an efficient terahertz detector [16]. In this paper, we have designed a non-contact and highly sensitive terahertz wave detector of sugar concentration with the $\text{Co}_3\text{Sn}_2\text{S}_2$ Weyl semimetal thin film, which can realize real-time and highly sensitive detection of blood sugar concentration to a certain extent.

2. Experimental setup and characterization

The preparation of the $\text{Co}_3\text{Sn}_2\text{S}_2$ thin film by magnetron sputtering is carried out as follows. Initially, the magnetron sputtering method is employed to optimize and establish the film preparation parameters for the $\text{Co}_3\text{Sn}_2\text{S}_2$ thin film. The aim is to achieve uniformity and high quality while minimizing defects. Through experimentation with various parameters, the following preparation steps are determined: reducing the air pressure to 1×10^{-4} Pa, introducing argon into the cavity, and depositing the $\text{Co}_3\text{Sn}_2\text{S}_2$ target in RF-driven mode. The parameters for the $\text{Co}_3\text{Sn}_2\text{S}_2$ thin film is specified as follows: argon flow rate of 50 SCCM, power of 120 W, and duration of 210 seconds. The electrode material is copper with a spacing of 5 mm.

Figure 1(a) shows the thickness of the $\text{Co}_3\text{Sn}_2\text{S}_2$ thin film is 166.7 nm. Figure 1(b) shows the design of this device experiment. Terahertz wave hits the surface of the detector, and the current is measured under the different concentrations solution. The experimental setup is consisted of a 70 mW, 0.1 THz avalanche diode (TeraSense IMPATT diodes) as a terahertz source, two tungsten probes, and a high-precision digital source meter (Keithley 2400) as shown in Fig. 1(c). The Raman spectrum of the film demonstrates the improved narrower and stronger Raman peaks, the E_g peak is located at 106 cm^{-1} and the $A_1 g$ peak is located at 151 cm^{-1} in Fig. 1(d).

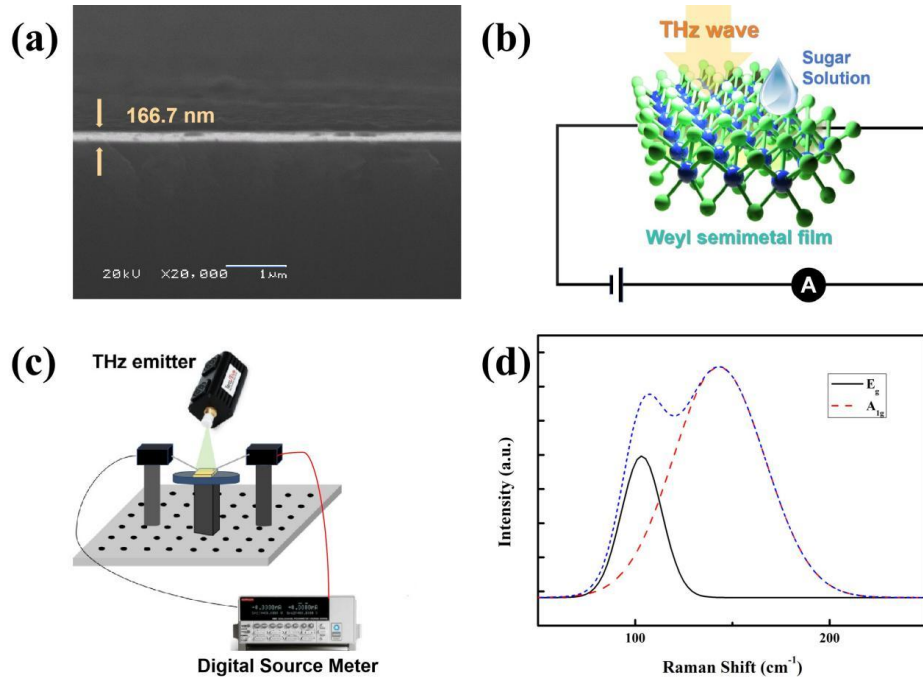


Fig. 1. Device design diagram. (a) Thickness of the $\text{Co}_3\text{Sn}_2\text{S}_2$ thin film. (b) Device experimental design diagram. (c) Experimental setup diagram. (d) Raman spectrum of the $\text{Co}_3\text{Sn}_2\text{S}_2$ thin film.

The terahertz detector is put in the center of the tungsten probe platform, the tips of the tungsten probes are used to contact with the detector's metal electrodes, and then changeable voltages of 9.8–11.6 V with 0.2 V interval is applied at both ends of the device to obtain dark current. After the dark current testing, terahertz wave of the terahertz source irradiates the surface of the device to obtain the light current at the different voltage. During the testing process, we need to keep the same position of the device in order to reduce measurement errors. Note that, the tungsten probes need to be grounded after each measurement to eliminate small static electricity, which affects the current results of subsequent tests.

3. Results and discussion

3.1. Detector excited only by terahertz wave

In order to more intuitively reflect the high performance of the terahertz detector with the $\text{Co}_3\text{Sn}_2\text{S}_2$ semimetal thin film, we firstly test the response parameters of the Si substrate-only terahertz detector. The Fig. 2(a) shows the relationship between the light current and the variable bias voltage at different concentrations of sugar solution. The current is linearly related to the voltage and gets smaller and smaller, as the concentration of the sugar solution increases. Current (I) can be written as:

$$I = \frac{nVe}{t} \quad (1)$$

n is the charge-carrier density, V is the volume, e is the elementary charge (1.602×10^{-19} C), and t is the transition time. Since the sugar is a polymer compound that does not conduct electricity, the higher the sugar solution is, the lower the charge-carrier density (n) is. At the same voltage,

the parameters of V , t and e keep constant. Since the carrier concentration (n) is reduced, the current (I) can correspondingly get smaller as shown in Fig. 2(a).

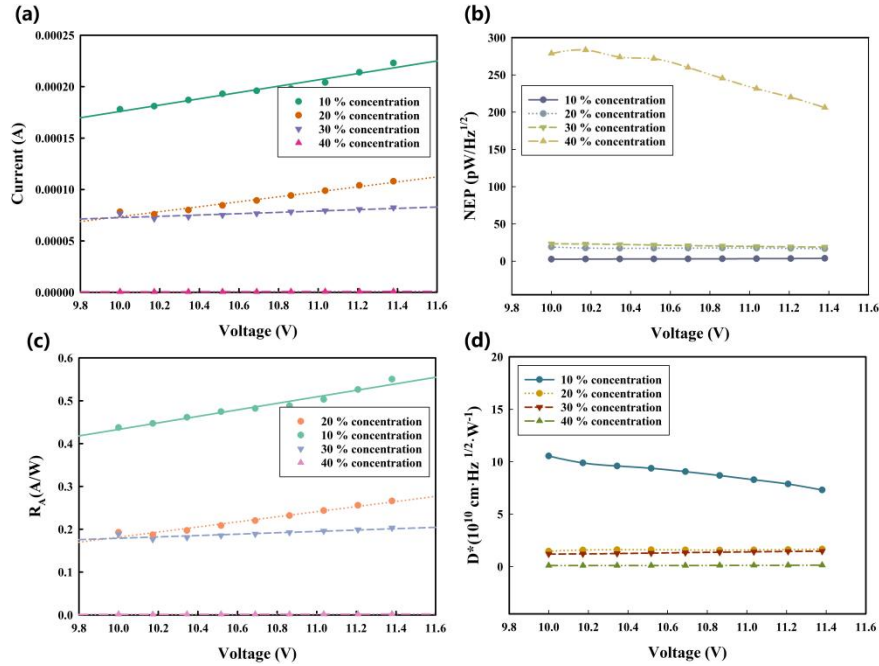


Fig. 2. Results of the Si substrate-only detector at different concentrations of sugar solution excited by terahertz wave. (a) Light Current. (b) NEP. (c) R_A . (d) D^* .

Figure 2(b)–(d) show the important parameters of the terahertz detector, such as the noise equivalent power (NEP), photo-responsivity (R_A) and detection rate (D^*). These parameters also can reflect the accurate concentration of the different sugar solutions.

The photo-responsivity (R_A) is defined as the light current (I) under the unit optical power (P), and expressed in the following equation [17,18]:

$$R_A = \frac{I}{P} \quad (2)$$

The noise equivalent power (NEP) can evaluate the sensitivity of the detector, and NEP represents the smallest detection optical power. The smaller the value of NEP is, the better its ability of the detection optical signal is [17,18]:

$$NEP = \frac{\nu_n}{R_A} \quad (3)$$

ν_n is the total noise, which can be categorized into thermal Johnson-Nyquist noise (ν_t) and dark current breakdown noise (ν_b) [19–21]:

$$\nu_n = \sqrt{\nu_t^2 + \nu_b^2} = \sqrt{4k_B T r + 2q I_d r^2} \quad (4)$$

k_B , T , r , q , and I_d are the Boltzmann constant, the absolute temperature, the resistance, the elementary charge, and the dark current of the device, respectively.

Detection rate (D^*) is the detector's normalized signal-to-noise ratio. It is closely related to the NEP. The smaller the NEP is, the higher the D^* is, and the better the detection performance

of the device is. D^* is defined as follows [17,18]:

$$D^* = \frac{\sqrt{S}}{NEP} \quad (5)$$

S is the effective detection area of this detector.

As shown in Fig. 2(a), the light current varies only 50–250 μA . We select the voltage of 11 V for specific analysis. When the concentration of sugar solution is 10%, the detector's light current is only 200 μA . As the concentration of sugar solution rises, the light current continues to decline. At the concentration of 30%, the light current value is less than 100 μA . As a result, when the concentration of sugar solution reaches 40%, the terahertz detector has been unable to test the accurate light current, i.e., the current remains 0 A as shown in Fig. 2(a).

At the voltage of 11 V and the concentration of 10%, the R_A and D^* of the detector are 0.5 A/W and $8.57 \times 10^{10} \text{ cm Hz}^{1/2} \text{ W}^{-1}$, respectively, and both decrease as the concentration of the concentrated solution increases as shown in the Fig. 2(a)–2(b). Compared with R_A and D^* , NEP decreases with increasing concentration of sugar solution. As shown in Fig. 2, when the sugar solution concentration is 40%, NEP reaches 230 $\text{pW/Hz}^{1/2}$ at 11 V, which is not an ideal value for a practical detector. Furthermore, due to the non-ideal precision of the detector, specific values cannot be measured when the sugar solution concentration is below 40% as the NEP approaches zero.

In summary, blood sugar testing can be completed by testing the response of terahertz wave to sugar solution of different concentrations. However, the Si substrate-only detector cannot complete the testing of high-concentration sugar solution due to its insufficient accuracy. Therefore, Weyl semimetal thin film is selected in the following to improve the performance.

The measurement process of the detector with the $\text{Co}_3\text{Sn}_2\text{S}_2$ film is basically the same as the Si substrate-only detector, and the conclusion that the light current decreases with the increase of sugar solution concentration is still valid. As shown in Fig. 3, the key parameters of the detector are significantly better than Si substrate-only detector after the addition of Weyl semimetal thin film. The light current can reach 5–35 mA at the voltage of 9.8–11.6 V, much larger than the former 50–250 μA . Taking the voltage of 11 V as an example, when the concentration of the sugar solution is 10%, the light current, R_A , and D^* are 27 mA, 68.6 A/W, and $38.3 \times 10^{10} \text{ cm Hz}^{1/2} \text{ W}^{-1}$, which are 134, 136.2, and 3.5 times higher than the Si substrate-only detector, respectively. In addition, the NEP is only 2.16 $\text{pW/Hz}^{1/2}$ at the sugar solution concentration of 40%, which is 105.5 times better than the 230 $\text{pW/Hz}^{1/2}$ of the previous detector.

Single Si substrate is unable to accurately measure the response of highly concentrated sugar solution due to its low precision. Fortunately, the detector with the $\text{Co}_3\text{Sn}_2\text{S}_2$ thin film is able to accurately measure the light current, R_A , D^* , and NEP after sugar solution of up to 40%. Therefore, it is feasible to use this detector for non-invasive blood sugar testing.

3.2. Detector simultaneously excited by a terahertz wave and laser

In order to further verify the reliability of the detector, 520 nm laser is used to stimulate the different concentrations of solution. The results follow the same trend as the above terahertz wave, i.e., the higher the concentration of the sugar solution is, the fewer photo-carriers are produced, and ultimately the lower current is obtained.

The Si substrate-only detector is still tested firstly. Figure 4 shows the dark and light currents of this detector under 520 nm laser irradiation. As the concentration of sugar solution increases, both the dark and light currents all decrease, which is similar to the results of the above terahertz response experiment. In addition, at the voltage of 11 V and the sugar solution concentration of 10%, the dark and light currents are very close to each other, both at around 240 μA . Furthermore, due to both synchronous excitation of terahertz and laser sources, the light current value is larger than the 200 μA as measured in 3.1.

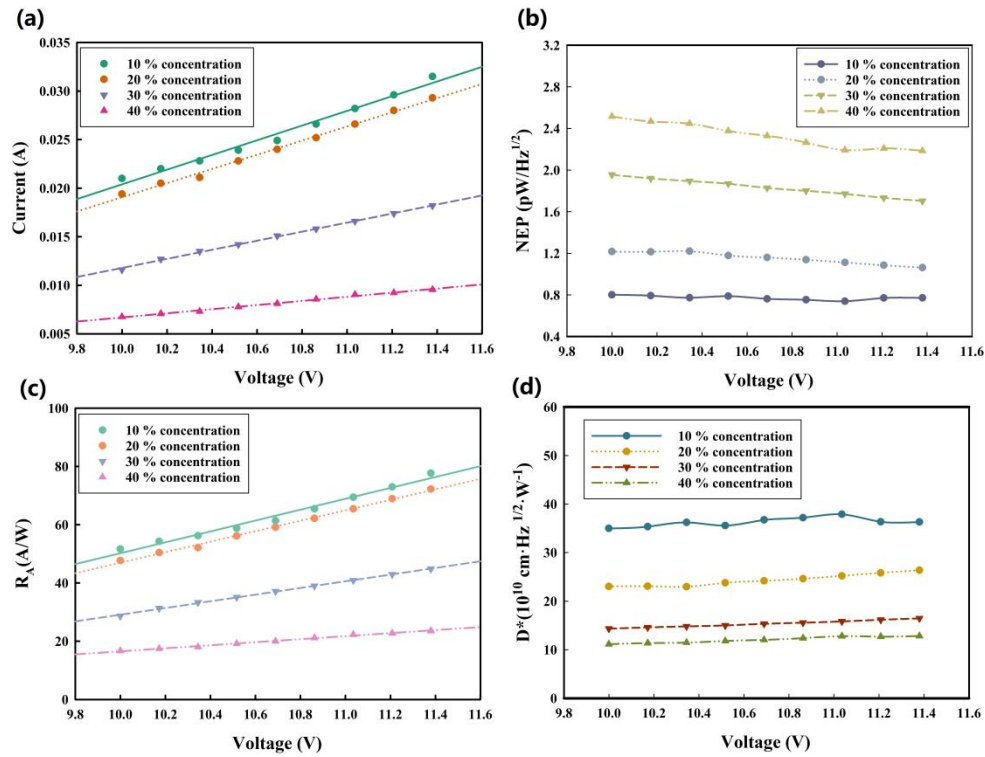


Fig. 3. Results of the detector with the $\text{Co}_3\text{Sn}_2\text{S}_2$ thin film at different concentrations of sugar solution excited by terahertz wave. (a) Light Current. (b) NEP. (c) R_A . (d) D^* .

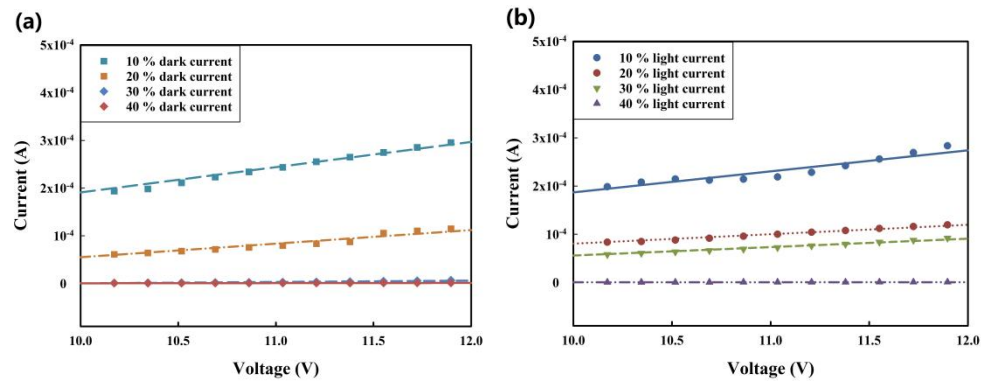


Fig. 4. Dark and light currents of the Si substrate-only detector at different concentration of sugar solution excited by 520 nm laser. (a) Dark Current. (b) Light Current.

However, this detector has the same problem as the Si substrate-only detector as mentioned in 3.1. As shown in Fig. 4, when the concentration of the sugar solution reaches 30%, the dark current of the detector cannot be detected, but the light current can still be measured because it is originated from the light stimulation and some spontaneous electron movement still exists in the device. Therefore, we choose the detector with the $\text{Co}_3\text{Sn}_2\text{S}_2$ semimetal thin film again to improve this experiment.

Figure 5 shows the dark and light currents generated by the detector with the $\text{Co}_3\text{Sn}_2\text{S}_2$ thin film under the bias voltage of 10–12 V. Taking the 11 V as an example, the light current of the 10% concentration sugar solution is about 30 mA, larger than the 18 mA of the dark current. When the solution concentration reaches 40%, the light current is only about 7 mA. Compared with the Si substrate-only detector, the detector with the $\text{Co}_3\text{Sn}_2\text{S}_2$ thin film not only detects the terahertz response of the high concentration sugar solution, but also the light current is significantly larger than the dark current, which shows that this device has a perfect response to external light. Therefore, it is very useful to fabricate blood sugar testing device for non-invasive testing of blood sugar.

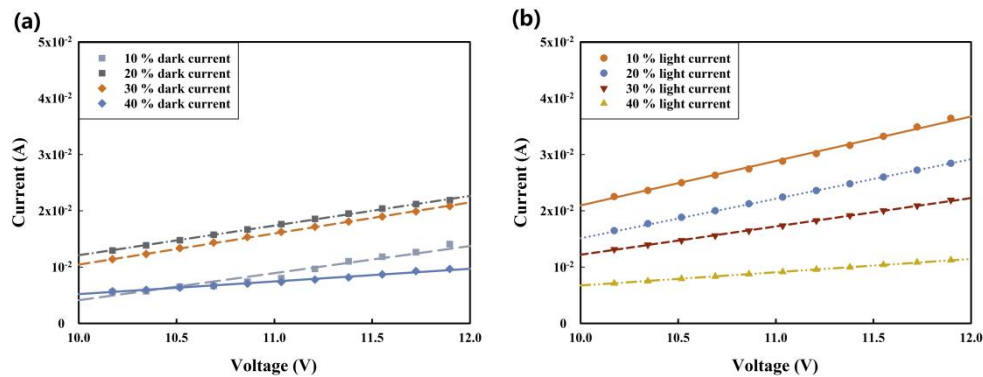


Fig. 5. Dark and light currents of the detector with the $\text{Co}_3\text{Sn}_2\text{S}_2$ thin film at different concentrations of sugar solution excited by 520 nm laser. (a) Dark Current. (b) Light Current.

In summary, the aforementioned four experiments mutually support the same finding: specifically, that the greater the concentration of the sugar solution is, the lower the current is. This conclusion may be utilized to infer the concentration of the sugar solution for the advancement of non-invasive blood sugar testing. Furthermore, the study also indicates that the detector with the $\text{Co}_3\text{Sn}_2\text{S}_2$ thin film exhibits a superior response to terahertz wave compared to the Si substrate-only detector, thereby enhances its ability to detect faint signals, indicates a heightened sensitivity in detecting blood sugar levels.

4. Conclusion

Non-invasive blood sugar testing has received a lot of attention, however, the non-invasive blood sugar testing currently has certain shortcomings that prevent it from being accommodated in the marketplace. In this paper, we propose a non-invasive blood sugar testing based on terahertz wave detection. It demonstrates not only the feasibility of non-invasive measurement of blood sugar with terahertz wave, but also the higher response of the detector to terahertz wave due to the Weyl semimetal thin film to increase the sensitivity. In order to confirm the reliability of the conclusions, we also choose laser simulation experiments for mutual verification. Furthermore, this detector can also be combined with deep learning and artificial intelligence and then creates a blood sugar testing device. In future, this device can be further expanded to 6 G edge intelligence

to complete non-invasive and real-time monitoring of blood sugar, and finally promote the development of 6 G technology.

Funding. National Natural Science Foundation of China (12104314, 62205136, 62205219); Natural Science Foundation of Fujian Province (2021J011217); Science Technology Innovation Plans of Xiamen (2022CXY04012); Technique Plans of Longyan City (2022LYF9017).

Disclosures. The authors declare that they have no known competing financial interests or personal relationships that could have appeared to influence the work reported in this paper.

Data availability. Data will be made available on request.

References

1. M. Li, R. Singh, C. Marques, *et al.*, "2D material assisted SMF-MCF-MMF-SMF based LSPR sensor for creatinine detection," *Opt. Express* **29**(23), 38150–38167 (2021).
2. L. Tang, S. J. Chang, C.-J. Chen, *et al.*, "Non-invasive blood glucose monitoring technology: A review," *Sensors* **20**(23), 6925 (2020).
3. S. R. Chinnadayyal, I. Park, and S. Cho, "Nonenzymatic determination of sugar at near neutral pH values based on the use of nafion and platinum black coated microneedle electrode array," *Microchim. Acta* **185**(5), 250 (2018).
4. V. S. Chaudhary, D. Kumar, and S. Kumar, "Gold-immobilized photonic crystal fiber-based SPR biosensor for detection of malaria disease in human body," *IEEE Sens. J.* **21**(16), 17800–17807 (2021).
5. G. Purvinis, B. D. Cameron, and D. M. Altrogge, "Noninvasive polarimetric-based sugar monitoring: An in vivo study," *J. Diabetes Sci. Technol.* **5**(2), 380–387 (2011).
6. B. H. Malik and G. L. Coté, "Characterizing dual wavelength polarimetry through the eye for monitoring sugar," *Biomed. Opt. Express* **1**(5), 1247–1258 (2010).
7. B. H. Malik and G. L. Coté, "Modeling the corneal birefringence of the eye toward the development of a polarimetric sugar sensor," *J. Biomed. Opt.* **15**(3), 037012 (2010).
8. R. J. McNichols and G. L. Cote, "Optical sugar sensing in biological fluids: An overview," *J. Biomed. Opt.* **5**(1), 5–16 (2000).
9. M. Li, R. Singh, M. S. Soares, *et al.*, "Convex fiber-tapered seven core fiber-convex fiber (CTC) structure-based biosensor for creatinine detection in aquaculture," *Opt. Express* **30**(8), 13898–13914 (2022).
10. Y. T. Lan, Y. P. Kuang, L. P. Zhou, *et al.*, "Noninvasive monitoring of blood glucose concentration in diabetic patients with optical coherence tomography," *Laser Phys. Lett.* **14**(3), 035603 (2017).
11. J. L. C. Perez, J. Gutiérrez-Gutiérrez, C. P. Mayoral, *et al.*, "Fiber optic sensors: A review for glucose measurement," *Biosensors* **11**(3), 61 (2021).
12. G. Li, Q. Xu, R. Singh, *et al.*, "Graphene oxide/multiwalled carbon nanotubes assisted serial quadruple tapered structure-based LSPR sensor for glucose detection," *IEEE Sens. J.* **22**(17), 16904–16911 (2022).
13. N. Morali, R. Batabyal, P. K. Nag, *et al.*, "Fermi-arc diversity on surface terminations of the magnetic Weyl semimetal $\text{Co}_3\text{Sn}_2\text{S}_2$," *Science* **365**(6459), 1286–1291 (2019).
14. J. Coulter, G. B. Osterhoudt, C. A. C. Garcia, *et al.*, "Uncovering electron-phonon scattering and phonon dynamics in type-I Weyl semimetals," *Phys. Rev. B* **100**(22), 220301 (2019).
15. S. Chi, Z. Li, Y. Xie, *et al.*, "A wide-range photosensitive Weyl semimetal single crystal-TaAs," *Adv. Mater.* **30**(43), 1801372 (2018).
16. Q. Song, Y. Xu, F. Gao, *et al.*, "MoTe₂ covered polarization-sensitive THz modulator toward 6 G technology," *IEEE Trans. Electron Devices* **70**(9), 4935–4939 (2023).
17. V. S. Chaudhary, D. Kumar, G. P. Mishra, *et al.*, "Plasmonic biosensor with gold and titanium dioxide immobilized on photonic crystal fiber for blood composition detection," *IEEE Sensors J.* **22**(9), 8474–8481 (2022).
18. Q. Song, Z. Zhou, G. Zhu, *et al.*, "Microdisk array based Weyl semimetal nanofilm terahertz detector," *Nanophotonics* **11**(16), 3595–3602 (2022).
19. S. Kumar, Y. Wang, M. Li, *et al.*, "Plasmon-based tapered-in-tapered fiber structure for p-cresol detection: From human healthcare to aquaculture application," *IEEE Sensors J.* **22**(19), 18493–18500 (2022).
20. Q. Song, Y. Zhou, E. S. Jia, *et al.*, "Large area crystalline Weyl semimetal with nano Au film based micro-fold line array for THz detector," *Sci. China Technol. Sci.* **66**(11), 3267–3275 (2023).
21. B. Kaur, S. Kumar, and B. K. Kaushik, "Recent advancements in optical biosensors for cancer detection," *Biosens. Bioelectron.* **197**, 113805 (2022).